

**SYNTHESIS AND CHARACTERIZATION OF MAGNETITE AND
MAGNETITE-EPOXY POLYMERS NANOCOMPOSITES AND
THEIR THERMAL AND ELECTRICAL BEHAVIORS**

by

TAN WEI LENG

**Thesis submitted in fulfillment of the requirements
for the degree of
Master of Science**

August 2007

ACKNOWLEDGEMENTS

I would like to take this opportunity to extend my heartiest appreciation to many people who have made it possible for me to complete this thesis.

First of all, I would like to thank Assoc. Prof. Mohamad Abu Bakar, my beloved supervisor for his tremendous guidance, advice, encouragement and most importantly supporting me throughout the completion of this work.

Our helpful and most dedicated lab assistants and staffs – Mr. Ali, Mr. Sobri, Mr. Burhanudin, Mr. Simon Aw Yeong, Mr. Yee and Mrs. Saripah from School of Chemical Sciences, Mr. Muthu, Miss Jamilah and Mr. Johari from the Electron Microscope Department, School of Biological Sciences, as well as Mr. Karuna, Mr. Kong and Mr. Mokhtar from School of Physics. A special thanks to all of them for their kind assistance in making my project a success.

Special thanks also go to all my friends who have assisted me in various aspects. Last but not least, my heartfelt appreciation also goes to my lovely family everlasting support.

Thank you.

TAN WEI LENG

August 2007

CONTENTS

| | Page |
|---|-------|
| Acknowledgements | ii |
| Contents | iii |
| List of Tables | vii |
| List of Figures | viii |
| List of Plates | xii |
| List of Symbols | xiii |
| List of Abbreviations | xiv |
| Abstrak | xvi |
| Abstract | xviii |
| | |
| CHAPTER 1 – INTRODUCTION | |
| 1.1 Brief Overview | 1 |
| 1.2 Research Objectives | 2 |
| 1.3 Scope of Study | 3 |
| 1.4 Thesis Layout | 3 |
| 1.5 References | 5 |
| | |
| CHAPTER 2 - LITERATURE REVIEW | |
| 2.1 Introduction to Nanoworld | 6 |
| 2.2 Nanoscience | 6 |
| 2.3 Nanomaterials | 9 |
| 2.4 Nanoparticles; Preparation, Size and Morphology | 12 |
| 2.5 Additives/Stabilizers/Matrices/Supports | 12 |
| 2.5.1 Surfactants | 13 |
| 2.5.2 Polymers | 14 |
| 2.5.3 Ligands | 15 |
| 2.5.4 Dendrimers | 15 |
| 2.5.5 Matrices/Supports | 16 |
| 2.6 Application of Nanomaterials | 16 |
| 2.6.1 Catalysts | 16 |
| 2.6.2 Biomedical | 17 |
| 2.6.3 Electronic and Magnetic | 17 |
| 2.6.4 Enviromental/Green Chemistry | 18 |
| 2.7 Metal Oxides | 18 |

| | | |
|---------|--|----|
| 2.7.1 | Importance of Metal Oxides | 18 |
| 2.7.2 | General Synthetic Routes to Metal Oxides Nanoparticles | 19 |
| 2.8 | Iron Oxides | 22 |
| 2.8.1 | Properties of Iron Oxides | 24 |
| 2.8.2 | Magnetite Nanoparticles | 25 |
| 2.8.2.1 | Preparation and Phase Transformation of Magnetite | 26 |
| 2.8.2.2 | Preparations of Polymer -stabilized and -supported Magnetite Nanoparticles | 28 |
| 2.9 | Epoxy Polymers | 29 |
| 2.9.1 | DGEBA Epoxy Resin | 30 |
| 2.9.1.1 | Hardener/Curing Agents | 30 |
| 2.9.2 | Epoxidized Natural Rubber | 31 |
| 2.10 | Liquid to Liquid Phase Transfer | 32 |
| 2.11 | Particles Dispersion | 33 |
| 2.11.1 | Fractal Method | 34 |
| 2.12 | References | 35 |

CHAPTER 3 - MATERIALS AND EXPERIMENTAL METHODS

| | | |
|---------|---|----|
| 3.1 | General | 45 |
| 3.2 | Materials | 45 |
| 3.3 | Experimental Methods for Chapter 4 | 46 |
| 3.3.1 | Synthesis of Magnetite via Alkaline Precipitation Method | 46 |
| 3.3.2 | Synthesis of Magnetite via Liquid to Liquid Phase Transfer Method | 46 |
| 3.3.2.1 | Two-step Method | 46 |
| 3.3.2.2 | One-step Method | 47 |
| 3.4 | Experimental Methods for Chapter 5 | 47 |
| 3.4.1 | Preparation of Magnetite-Epoxy Polymers Nanocomposites | 47 |
| 3.5 | Experimental Methods for Chapter 6 | 48 |
| 3.5.1 | Preparation of Magnetite-DGEBA/MDA Nanocomposites | 48 |
| 3.5.2 | Preparation of DGEBA/MDA Composite | 49 |
| 3.6 | Experimental Methods for Chapter 7 | 49 |
| 3.6.1 | Preparation of Magnetite-ENR-50/PEO Nanocomposite | 49 |
| 3.6.2 | Preparation of ENR-50/PEO Composite | 49 |
| 3.7 | Equipments and Characterizations | 50 |

| | | |
|-------|--|----|
| 3.7.1 | Transmission Electron Microscope (TEM) | 50 |
| 3.7.2 | Scanning Electron Microscope (SEM) | 50 |
| 3.7.3 | Fourier Transform Infrared (FTIR) Spectroscopy | 51 |
| 3.7.4 | Powder X-ray Diffraction (XRD) Technique | 51 |
| 3.7.5 | Atomic Absorption Spectroscopy (AAS) | 51 |
| 3.7.6 | Gel Permeation Chromatography (GPC) | 51 |
| 3.7.7 | Differential Scanning Calorimetry (DSC) | 52 |
| 3.7.8 | Thermogravimetric Analysis (TGA) | 52 |
| 3.7.9 | Electrical Conductivity Measurement | 52 |
| 3.8 | References | 54 |

CHAPTER 4 - SYNTHESIS AND CHARACTERIZATION OF MAGNETITE NANOPARTICLES

| | | |
|---------|---|----|
| 4.1 | Introduction | 55 |
| 4.2 | Synthesis of Magnetite via Alkaline Precipitation Method | 56 |
| 4.2.1 | Additive-stabilized Magnetite | 57 |
| 4.2.1.1 | Characterizations | 57 |
| 4.2.1.2 | Particles Size and Morphology | 59 |
| 4.3 | Synthesis of Magnetite via Liquid to Liquid Phase Transfer Method | 65 |
| 4.3.1 | Preliminary Works | 65 |
| 4.3.2 | The Synthesis | 66 |
| 4.3.3 | Characterizations | 67 |
| 4.3.4 | Particles Transfer Efficiency, Size and Morphology | 70 |
| 4.3.5 | Mechanism of Particles Interphase Transfer | 73 |
| 4.4 | References | 76 |

CHAPTER 5 - SYNTHESIS AND CHARACTERIZATION OF MAGNETITE-EPOXY POLYMERS NANOCOMPOSITES

| | | |
|-------|--|----|
| 5.1 | Introduction | 79 |
| 5.2 | Synthesis and Characterizations | 80 |
| 5.2.1 | Synthesis, Organosol Stability and Transfer Efficiency | 80 |
| 5.2.2 | Characterizations | 84 |
| 5.3 | Size, Size Distribution and Morphology | 87 |
| 5.4 | The Nanocomposites Characteristics | 91 |
| 5.5 | References | 98 |

**CHAPTER 6 - THERMAL AND ELECTRICAL BEHAVIOR OF THE
CURED MAGNETITE-DGEBA NANOCOMPOSITES**

| | | |
|-----|--|-----|
| 6.1 | Introduction | 101 |
| 6.2 | Synthesis, Organosol Stability and Transfer Efficiency | 103 |
| 6.3 | Characterizations | 103 |
| 6.4 | Size, Size Distribution and Morphology | 106 |
| 6.5 | Thermal Behavior | 108 |
| 6.6 | Electrical Behavior | 111 |
| 6.7 | References | 117 |

**CHAPTER 7 - THERMAL AND ELECTRICAL BEHAVIOR OF
MAGNETITE-ENR-50/PEO NANOCOMPOSITES**

| | | |
|-----|--|-----|
| 7.1 | Introduction | 120 |
| 7.2 | Synthesis, Organosol Stability and Transfer Efficiency | 121 |
| 7.3 | Characterizations | 122 |
| 7.4 | Size, Size Distribution and Morphology | 125 |
| 7.5 | Thermal Behavior | 127 |
| 7.6 | Electrical Behavior | 132 |
| 7.7 | References | 135 |

CHAPTER 8 – CONCLUSION

| | | |
|-----|---------------------------------|-----|
| 8.1 | Research Summary | 138 |
| 8.2 | Recommendations for Future Work | 141 |

APPENDIX

| | | |
|--|--|------------|
| | Appendix 1 | 142 |
| | List of Publications and Presentations at Conferences | 143 |

LIST OF TABLES

| | Page | |
|-----------|--|-----|
| Table 2.1 | Size relationships of atoms/molecules, nanoparticles, and condensed matter | 7 |
| Table 2.2 | Some important classes of nanomaterials and their commercial applications | 8 |
| Table 2.3 | Some important terminology used in nanoscience | 9 |
| Table 2.4 | Various iron oxides | 23 |
| Table 2.5 | Magnetite nanoparticles synthesized by various methods and their respective stabilizer/matrixes | 26 |
| Table 3.1 | Experiment sets with various conditions | 48 |
| Table 4.1 | Size and IR band of magnetite particles prepared in various additives | 59 |
| Table 4.2 | The FTIR data (cm^{-1}) of CTAB and the variously prepared magnetite | 68 |
| Table 4.3 | Particles transfer efficiency, size and standard deviation (σ) of the variously prepared magnetite nanoparticles via phase transfer methods | 70 |
| Table 5.1 | The efficiency of magnetite particles transfer from aqueous to toluene phase containing the various % wt/wt of epoxy polymers | 82 |
| Table 5.2 | Assignments of FTIR peaks for the various magnetite-epoxy polymers nanocomposites | 86 |
| Table 5.3 | T_g values for neat epoxies and various magnetite-epoxy polymers composites | 87 |
| Table 5.4 | Particles size and standard deviation of the magnetite particles synthesized in different conditions | 94 |
| Table 5.5 | Loading factor of different components in composite at various % wt/wt | 96 |
| Table 6.1 | Comparison of fractal dimension, D value for magnetite in various matrices | 108 |
| Table 6.2 | T_g values for neat DGEBA, cured DGEBA resin and the cured 1% wt/wt magnetite-DGEBA /MDA composite | 109 |
| Table 7.1 | Melting temperature (T_m) and relative crystallinity (X_c) for PEO and its composites | 131 |

LIST OF FIGURES

| | Page | |
|-------------|---|----|
| Figure 2.1 | The relation between the total number of atoms in full shell clusters and the percentage of surface atoms | 10 |
| Figure 2.2 | Formation of a band structure (a) from a molecular state, (b) from a nanosized particle and (c) the fully developed band structure consisting of <i>s</i> and <i>d</i> band | 11 |
| Figure 2.3 | Mechanisms of the stabilization of nanoclusters by (a) electrostatic and (b) steric repulsion | 13 |
| Figure 2.4 | Microstructure arising from surfactant (1) monomers, (2) spherical micelle, (3-4) cylindrical micelles, (5) lamellar micelle and (6) water droplets packed as hexagons in the reverse micellar system | 14 |
| Figure 2.5 | Various generation (G4, G6, G8) of poly(amidoamine) dendrimers | 16 |
| Figure 2.6 | Typical steps for sol gel process | 20 |
| Figure 2.7 | Schulman's model for the reverse micelle | 21 |
| Figure 2.8 | Phase transformation between iron oxides | 27 |
| Figure 2.9 | Synthesis of iron oxides via various conditions | 27 |
| Figure 2.10 | Various fabrication routes of nanoparticles incorporated functional polymer | 29 |
| Figure 2.11 | Chemical structure for DGEBA epoxy resin | 30 |
| Figure 2.12 | Typical curing mechanism of epoxy resin with amine based hardener | 31 |
| Figure 2.13 | Chemical structure for ENR | 32 |
| Figure 3.1 | Experimental set-up for electrical conductivity measurement | 53 |
| Figure 4.1 | FTIR spectra (600-1100 cm^{-1}) of magnetite synthesized with and without additives | 57 |
| Figure 4.2 | Representative XRD patterns of magnetite prepared (a) with SDS, (b) with citrate, (c) without additive and (d) Reference (JCPDS File No 19-629) | 58 |
| Figure 4.3 | Size distribution of as-prepared magnetite particles in various additives | 62 |
| Figure 4.4 | TEM micrographs of magnetite particles prepared without additive | 62 |

| | | |
|-------------|---|----|
| Figure 4.5 | TEM micrographs of magnetite particles synthesized with (a) CTAB, (b) SDS, (c) TOPO, (d) triton X-100, (e) chitosan, (f) thiourea, (g) citrate and (h) stearic acid | 64 |
| Figure 4.6 | Plot of percentage of iron content in liquid phase versus various % (wt/wt) CTAB as transferring agent in the one-step phase transfer technique | 65 |
| Figure 4.7 | FTIR spectra for magnetite nanoparticles synthesized via (a) one-step method with (i) benzene, (ii) toluene, (iii) xylene and (iv) mesitylene as organic phase; (b) two-steps method (toluene) (i) before phase transfer and (ii) after phase transfer; (c) alkaline precipitation without additive | 68 |
| Figure 4.8 | XRD diffractograms of magnetite particles prepared via (a) one-step method (i) benzene, (ii) xylene, (iii) mesitylene, (iv) toluene and (b) two-steps method (toluene) and (c) magnetite (pure) reference database (JCPDS File No.19-629) | 69 |
| Figure 4.9 | Size distribution of the as-synthesized magnetite particles prepared with (a) one-step and two-step methods (both toluene phase) and (b) one step method with different organic solvents | 71 |
| Figure 4.10 | The correlation between the average particles' size and dipole moment | 72 |
| Figure 4.11 | TEM images of magnetite particles synthesis with one-step method (a) toluene (b) benzene (c) xylene (d) mesitylene and two-steps method (e) before (f) after transfer | 74 |
| Figure 4.12 | Schematic of reaction occurring in the water in oil micro-droplets system according to Summ and Ivanova | 75 |
| Figure 5.1 | Intermolecular interactions between C_n TAB and epoxy resin molecule | 83 |
| Figure 5.2 | Typical XRD diffractogram for (a) 1% wt/wt magnetite-DGEBA resin, (b) 1% wt/wt magnetite-ENR-50 and (c) magnetite data reference (JCPDS File No 19-629) | 84 |
| Figure 5.3 | FTIR spectra for magnetite prepared in (a) 1% wt/wt ENR-50, (b) 3% wt/wt ENR-50, (c) 1% wt/wt DGEBA and (d) 5% wt/wt DGEBA | 85 |
| Figure 5.4 | TEM images of magnetite-DGEBA nanocomposites at various % wt/wt DGEBA (a-b) 1%, (c-d) 10% | 88 |
| Figure 5.5 | TEM images of magnetite-ENR-50 nanocomposites at various % wt/wt ENR (a-b) 1%, (c-d) 3% | 88 |
| Figure 5.6 | SEM micrographs of (a-b) pure magnetite particles, magnetite particles in (c-d) 1% wt/wt DGEBA and (e-f) 1% wt/wt ENR-50 | 90 |

| | | |
|-------------|--|-----|
| Figure 5.7 | (a) Average size, standard deviation and (b) plot $\ln M$ versus $\ln r$ for magnetite particles prepared with different percentage of epoxy polymers | 91 |
| Figure 5.8 | The destruction of microdroplets upon further addition of epoxy | 93 |
| Figure 5.9 | TEM images of magnetite-DGEBA (10% wt/wt) nanocomposites prepared with 20% wt/wt CTAB at (a) high and (b) low magnification [first modification] | 94 |
| Figure 5.10 | TEM images of 1% (wt/wt) (a) magnetite-DGEBA composites and (b) magnetite-ENR-50 composites re-dispersed in n-hexane | 97 |
| Figure 6.1 | FTIR spectra for (a) neat DGEBA, (b) cured DGEBA/MDA and (c) cured magnetite-DGEBA/MDA composite | 105 |
| Figure 6.2 | Typical crosslinking reaction between DGEBA and MDA curing agent [where R = alkyl or aryl] | 105 |
| Figure 6.3 | TEM images for (a-b) 1% wt/wt and (c-d) 10% wt/wt DGEBA epoxy resin-magnetite nanocomposites prepared with MDA curing agent | 107 |
| Figure 6.4 | TG and DTG curves for neat DGEBA, DGEBA/MDA and 1% wt/wt magnetite-DGEBA/MDA composite | 110 |
| Figure 6.5 | Temperature dependence of specific volume resistivity, $\rho(T)$ DGEBA/MDA composite, 1% wt/wt magnetite-DGEBA/MDA composite and pure magnetite | 112 |
| Figure 6.6 | Schematic of the reduction of interparticle distance upon heating | 114 |
| Figure 6.7 | First and second DSC heating scan for magnetite-DGEBA/MDA composite | 116 |
| Figure 7.1 | XRD pattern for (a) magnetite-ENR-50/PEO composite and (b) magnetite-PEO composite and (c) pure PEO | 123 |
| Figure 7.2 | FTIR spectra for (a) neat PEO, (b) ENR-50/PEO blend, (c) magnetite-ENR-50/PEO composite and (d) magnetite-PEO composite | 125 |
| Figure 7.3 | TEM images of (a-b) magnetite-ENR-50/PEO composite and (c-d) magnetite/PEO composite | 127 |
| Figure 7.4 | TG and DTG curves for neat ENR-50, neat PEO, 1:1 weight ratio ENR-50/PEO, 1% wt/wt magnetite-ENR-50/PEO composite and 1% wt/wt magnetite-PEO composite | 128 |
| Figure 7.5 | DSC thermograms for neat PEO, 1:1 weight ratio ENR-50/PEO blend, 1% wt/wt magnetite-ENR-50/PEO and 1% wt/wt magnetite-PEO composite | 131 |

Figure 7.6 Temperature dependence of specific volume resistivity, $\rho(T)$ of neat PEO, 1:1 weight ratio ENR-50/PEO blend, 1% wt/wt magnetite-ENR-50/PEO composite, 1% wt/wt magnetite-PEO composite and pure magnetite 132

LIST OF PLATES

| | | Page |
|-----------|---|------|
| Plate 4.1 | Photographs of one-step phase transfer reaction progress | 67 |
| Plate 5.1 | Typical sedimentation of magnetite particles as exemplified by (10% wt/wt) magnetite-DGEBA organosol (a) upon preparation and (b) a day after preparation | 82 |
| Plate 7.1 | Digital images for magnetite-ENR-50/PEO organosols prepared (a) with modification and (b) without modification | 122 |

LIST OF SYMBOLS

| | |
|------------|------------------------------------|
| 2θ | Bragg angle |
| σ_i | Ionic conductivity |
| σ_e | Electronic conductivity |
| R | Radius |
| w | Molar ratio of water to surfactant |
| wt/wt | Weight to weight ratio |
| D | Dipole moment |
| T_g | Glass transition temperature |
| ρ (T) | Specific volume resistivity |

LIST OF ABBREVIATIONS

| | |
|--------------|--|
| AAS | Atomic absorption spectroscopy |
| α -CD | α -cyclodextrin |
| CMC | Critical micelle concentration |
| CNT | Carbon Nanotube |
| CTAB | Cetyltrimethylammonium bromide |
| DDAC | Dimethyldioctadecylammonium chloride |
| DDM | 4,4-diaminophenylmethane |
| DGEBA | Diglycidyl ether of bisphenol A |
| DOS | Density of state |
| DSC | Differential scanning calorimeter |
| E_F | Fermi Energy |
| EC | Ethylene carbonate |
| ENR | Epoxidized natural rubber |
| ENR-50 | Epoxidized natural rubber with 50% epoxidation |
| FTIR | Fourier transform infrared |
| GPC | Gel Permentation Chromatography |
| HDEHP | Bis(ethylhexyl)hydrogen phosphate |
| HOMO | High occupied molecular orbital |
| LUMO | Low unoccupied molecular orbital |
| MDA | Bis-(4-aminophenyl)methane |
| MRI | Magnetic resonance imaging |
| PAA | Polyacrylic acid |
| PAMAM | Poly(amidoamine) |
| PC | Propylene carbonate |
| PEO | Polyethylene oxide |
| PLGA | Poly(D, L-lactide-co-glycolide) |
| POE | Polyoxyethelyene |
| PVA | Poly(vinylalcohol) |
| PVCL | Poly-N-vinylcaprolactam |
| PVP | Polyvinylpyrrolidone |
| SD | Standard deviation |
| SDS | Sodium dodecyl sulfate |
| SLS | Sodium lauryl sulfate |
| SPR | Surface plasmon resonance |

| | |
|----------------|----------------------------------|
| SWNT | Single Wall Nanotube |
| T _g | Glass transition temperature |
| TEM | Transmission Electron Microscope |
| TGA | Thermogravimetric analysis |
| TOAB | Tetra-n-octyl-ammonium bromide |
| TOPO | Tri-n-octylphosphinoxide |
| UV | Ultraviolet |
| UV-vis | Ultraviolet-visible |
| W/O | Water-in-oil |
| XRD | X-ray diffraction |

SINTESIS DAN PENCIRIAN MAGNETIT DAN NANOKOMPOSIT MAGNETIT-POLIMER EPOKSI SERTA KELAKUAN TERMA DAN ELEKTRIKNYA

ABSTRAK

Nanozarah magnetit (Fe_3O_4) disintesis melalui pemendakan beralkali. Kesan pelbagai aditif dan persekitaran akues-organik terhadap saiz, keseragaman saiz dan morfologi zarah magnetit dikaji. Kajian ini diikuti dengan penyediaan magnetit-polimer epoksi organosol dan serbuk nanokomposit masing-masing melalui teknik pemindahan fasa akues ke toluena. Dua polimer epoksi yang digunakan adalah diglisidil eter bisfenol A (DGEBA) dan getah asli 50 % terepoksida (ENR-50). Akhirnya, komposit ternari diperolehi melalui penambahan bis-(4-aminofenil)metana (MDA) dan poli(etilena oksida) (PEO) kepada komposit magnetit-DGEBA dan magnetit-ENR-50 masing-masing. Kelakuan terma dan elektriknyanya dikaji. Corak pembelauan serbuk sinar-X dan spektrum IR untuk zarah magnetit yang disediakan mengesahkan ketulenan hasil melalui ketiadaan ferum oksida fasa-fasa lain seperti maghemit atau hematit dalam sampel. Analisis saiz dan taburan saiz zarah magnetit mencadangkan bahawa zarah yang terbentuk bergantung pada jenis aditif yang digunakan dan persekitaran fasa cecair semasa penyediaannya. Surfaktan memberi kawalan yang lebih baik terhadap saiz zarah (ca. <45 nm) dan juga taburan saiz (ca. SD <20 nm) bagi aditif yang digunakan. Kesan persekitaran akues-organik terhadap zarah magnetit dinilai melalui teknik pemindahan fasa cecair ke cecair yang melibatkan kaedah pemindahan satu- dan dua-langkah. Dalam kedua-dua kes, CTAB digunakan sebagai penstabil dan juga agen pemindahan. Didapati saiz dan taburan saiz zarah didorong oleh sifat semulajadi pembentukan magnetit dalam fasa akues. Dalam kaedah satu-langkah, purata saiz zarah dan SD adalah separuh daripada kaedah dua-langkah (ca. 18.3 ± 7.7 nm cf. 42.2 ± 17.6 nm). Pengurangan ini disebabkan oleh pembentukan air dalam setiap titisan minyak yang bertindak sebagai reaktor nano untuk sintesis zarah magnetit. Analisis FTIR dan XRD terhadap magnetit-polimer epoksi organosol

menunjukkan kehadiran magnetit dan juga CTAB dalam fasa organik. Interaksi antara CTAB dan polimer epoksi menyebabkan ketidakstabilan zarah – zarah mengakibatkan pengaglomeratan dan pemendakan zarah. Namun, kehadiran polimer epoksi tidak mengganggu peranan CTAB sebagai agen pemindahan yang ditunjukkan oleh keberkesanan pemindahan yang tinggi (ca. ~99%) berdasarkan analisis AAS. Komposit serbuk diperoleh selepas pengeringan pelarut. Mikrograf SEM komposit serbuk menunjukkan zarah magnetit yang wujud adalah halus, diskret dan diselaputi lapisan polimer epoksi. Bagi komposit ternari, magnetit dalam DGEBA/MDA mengganggu tindak balas pematangan dan menghalangnya daripada pematangan lengkap. Ini dibuktikan oleh kepersisan puncak oksiran dalam spektrum FTIR dan juga pengurangan nilai T_g melalui penentuan DSC. Selain itu, zarah magnetit juga bertindak sebagai pemplastik pepejal yang merencat penghabluran PEO. Analisis TGA menunjukkan pelbagai penguraian terjadi dalam komposit ternari. Penentuan kerintangan I-V komposit ternari mencadangkan kekonduksian elektronik adalah dominan pada julat suhu yang rendah manakala kekonduksian ionik dikawal oleh prestasi elektrik pada suhu sederhana.

SYNTHESIS AND CHARACTERIZATION OF MAGNETITE AND MAGNETITE-EPOXY POLYMERS NANOCOMPOSITES AND THEIR THERMAL AND ELECTRICAL BEHAVIORS

ABSTRACT

Magnetite (Fe_3O_4) nanoparticles are synthesized via alkaline precipitation. The effect of different additives and aqueous-organic environment on the size, size uniformity and morphology of magnetite particles is studied. This is followed by the magnetite-epoxy polymer organosols and their respective powdered nanocomposites prepared via the aqueous to toluene phase transfer technique. The two epoxy polymers used are diglycidyl ether of bisphenol A (DGEBA) and modified natural rubber at 50% epoxidation (ENR-50). Finally, ternary composites were obtained via the addition of bis-(4-aminophenyl)methane (MDA) and poly(ethylene oxide) (PEO) to the magnetite-DGEBA and magnetite-ENR-50 composites, respectively. Their thermal and electrical behaviors were studied. The X-ray powder diffraction patterns and IR spectra of the prepared magnetite particles confirmed the purity of the products via the absence of other phases of iron oxides such as maghemite or hematite in the samples. Analyses on the size and size distribution of the magnetite particles suggest that the as-formed particles are dependent on the types of additives used and the liquid phase environment during the preparation. Surfactants gave a better control on the particles size (ca. <45 nm) as well as size distribution (ca. SD <20 nm) amongst the additives that are used. The effect of aqueous-organic environment on the magnetite particles was evaluated via the liquid to liquid phase transfer techniques employing one- and two-step methods. In both cases, CTAB was used as both stabilizer and transferring agent. It was found that the size and size distribution of particles was governed by the nature of magnetite formation in the aqueous phase. In the one-step method, the average particles size and SD is half of that afforded in the two-step method (ca. 18.3 ± 7.7 nm cf. 42.2 ± 17.6 nm). This reduction of size is attributed to the formation of water

in oil droplets that acts as nanoreactors for the synthesis of magnetite particles. FTIR and XRD analyses of the magnetite-epoxy polymer organosols indicate the presence of magnetite particles as well as CTAB in the organic phase. The interactions between CTAB and epoxy polymers resulted in the destabilizing of the particles, hence the occurrence of particles agglomeration and sedimentation. Nonetheless, the presence of epoxy polymers does not obstruct the role of CTAB as the transferring agent indicated by the high transferring efficiency (ca. ~99%) based on AAS analyses. A powder composite was obtained upon the removal of solvent. SEM micrographs of the powdered composites revealed that the magnetite particles appeared to be fine, discrete and covered by a layer of epoxy polymers. For the ternary composites, the magnetite in the DGEBA/MDA hinders the curing reactions and prevents it from completion. This is evident by the persistence of oxirane peaks in the FTIR spectrum as well as a decrement of the T_g value in the DSC measurement. On the other hand, magnetite particles act as solid plasticizer which inhibits the crystallization of PEO. TGA analyses revealed that multiple degradations occurred in the ternary composites. The I-V resistivity measurements on the ternary composites suggest that the electronic conduction is dominant in the low temperature range whereas ionic conduction controls their electrical performances at moderate temperatures.

CHAPTER 1

INTRODUCTION

1.1 Brief Overview

Nanotechnology has emerged as one of the most exciting fields all around besides biotechnology. The extent of coverage of the scientific studies in this field includes understanding, fabrications and applications of materials, devices and systems of nanometer dimension(s). Scientific enthusiasm about the nature and possible applications of these nano-materials are revolutionizing and can bring much benefit all over. Today, this nanoscale technology has encompassed many disciplines such as electronic, computing, medicine, catalysis and the likes. The nanosized materials showed different properties from their bulk matter due to the quantum size effect ¹. Thus, these have opened the door to the development of high performance materials with attractive properties. The properties of nanosized particles are strongly dependent on their size, morphology and preparative methods ². Thus the effort of synthesizing inorganic particles with reasonable particle size, narrower size distribution and consistent morphology is crucial to meet the demand tailored to certain functionality and or applications. These inorganics are those that are normally used or encountered in the everyday life which includes metals, their oxides and chalcogenides. One example of such inorganic material is the magnetite, Fe_3O_4 . Although there are numerous studies on synthesizing the magnetite particles, there is yet any report on the effect of different types of additives on the particle size, size distribution and morphology of the as-formed particles. Apart from that, there is also barely any reports on the synthesis of magnetite nanoparticles employing liquid-liquid phase transfer techniques. Inorganic-polymer composite is one of the recently focused materials worldwide by scientists and technologists alike. The anticipated enhance properties of these composite materials is their main objectives. This is coupled with the tremendous

growth of various industries requirements of high performance materials that has further driven their development. Inorganic-epoxy polymer based composites are one of the said interests as they can be applied as electrical conductive adhesive (ECA), thermal interface material (TIM), polyelectrolyte and the likes. These composites are said to exhibit an improve performance and properties adopted from either or both of the respective inorganic and organic composite components ³. Magnetite particles posses' high mechanical strength and is a semiconductor while the epoxy polymers are known reinforced materials with film-forming ability. Thus, the combination of both magnetite and epoxy polymers can be tailored to the thermal and electrical applications.

1.2 Research Objectives

The followings are the objectives of this study:

- To synthesize and characterize magnetite (Fe_3O_4) nanoparticles with reasonable particles size and size distribution using the simplest preparative method – alkaline precipitation
- To study the effect of additives and aqueous-organic environment on the particles size, size distribution and morphology of the as-formed magnetite nanoparticles
- To synthesize and characterize magnetite-epoxy polymer binary nanocomposites
- To study the effect and type of the epoxy polymers used on the dispersion stability, particles size and morphology of the magnetite nanoparticles
- To investigate the thermal and electrical behaviors of the magnetite-DGEBA/MDA and magnetite-ENR-50/PEO ternary composites

1.3 Scope of Study

The research is limited to the synthesizing of magnetite nanoparticles and magnetite-epoxy based nanocomposites via chemical routes. The simplest method, viz. alkaline precipitation and the adaptation to the liquid-liquid phase transfer techniques is chosen in this study. An evaluation with respect to the particles size, size distribution and morphology of the as-formed magnetite particles is performed. In the second part of the study, the preparation of magnetite-epoxy polymers based binary composites is carried out in view of the characteristic properties of both inorganic and organic components in the composites while sustaining the size as well as morphology of the particles. The epoxy polymers employed in this study are the diglycidyl ether of bisphenol A (DGEBA) epoxy resin and the epoxidized natural rubber with 50% epoxidation (ENR-50) due to some special properties they offer. Finally, the study focuses on the thermal and electrical properties of the epoxy polymer-coated magnetite ternary composites.

1.4 Thesis Layout

This thesis comprises of eight chapters. Chapter 1 is an overview of the thesis. The problem statements, the scope of study and research objectives are included. Chapter 2 presents a literature review on the related subjects and the development of the related fields. In Chapter 3, the detail methodology and techniques of characterization are described. Chapter 4 presents the synthesis and characterization of magnetite nanoparticles while Chapter 5 covers the synthesis and characterization of magnetite particles in the presence of epoxy polymers. Two types of epoxy polymers are chosen, namely diglycidyl ether of bisphenol A epoxy resin (DGEBA) and epoxidized natural rubber with 50% epoxidation (ENR-50). The effect of these epoxy polymers on the morphology, particle size and size distribution of the as-formed magnetite particles is discussed. Chapter 6 and 7 focused on the thermal and electrical behavior of magnetite particles in epoxy polymer-based systems. Bis-(4-

aminophenyl)methane (MDA) and poly(ethylene oxide) (PEO) is added to DGEBA and ENR-50 respectively. As the conclusion, the overall summary of the research findings and future works is addressed in the last Chapter 8.

1.5 References

1. L. M. Liz-Marzan and A. P. Philipse, Stable Hydrosols of Metallic and Bimetallic Nanoparticles Immobilized on Imogolite Fibers, *J. Phys. Chem.*, **99**, 15120, 1995.
2. D. Wang, C. Song, G. Gu and Z. Hu, Preparation of Fe₂O₃ Microcages from the Core/Shell Structures. *Mater. Lett.*, **59**, 782, 2005.
3. X. F. Qian, J. Yin, Y. F. Yang, Q. H. Liu, Z. K. Zhu and J. Lu, Polymer-inorganic Nanocomposites Prepared by Hydrothermal Method: Preparation and Characterization of PVA-Transition Metal Sulfides, *J. Appl. Polym. Sci.*, **82**, 2744, 2001.

CHAPTER 2

LITERATURE REVIEW

2.1 Introduction to Nanoworld

The concept of “nano” dated back to the year 1959 when a physicist Richard Feynman introduced the idea in a nobel lecture entitled “There’s plenty of room at the bottom” ¹. In this, he stressed that materials can be formed by manipulating individual atoms. He also predicted that nanotechnology will bring about a scientific revolution in the next century. Today, more than 40 years later, his vision becomes a reality whereby more and more nano-based technologies are being applied in our everyday lives. As an example, Samsung Company is the pioneers in marketing products such as washing machines and refrigerators incorporating nanosized silver as antimicrobial agents. Other scientists or researchers have also hinted the birth of this revolutionary technology. One of the co-founders of Intel Corporation, Gordon E. Moore, predicted that the number of transistors on a computer chip will double in every 18 months. What this means is that people are looking for finer structures for future technological applications. This prediction is now well known as the “Moore’s Law” ². Therefore it is obvious that in order to response to the need in developing fine and miniature devices, nanoscience has become a vital and exciting field. This area not only focuses on technology applications but also fundamental understanding.

2.2 Nanoscience

Quantum chemistry is the study of matter at an atomic or molecular level, whereas the condensed matter which generally consists of more than 10^6 atoms/molecules is the realm of the solid state chemistry. As for the particle which falls in the size range of 1-100 nm, neither quantum nor solid state chemistry can be used satisfactorily to explain the phenomena they exhibit. The particles in this regime are too large to be deemed as molecules, but too small to be considered as bulk

Table 2.2: Some important classes of nanomaterials and their commercial applications⁷

| Material class | Applications |
|--|---|
| 1. Buckly balls and CNTs | Production of SWNTs, gas sensors, memory chips (RAM), nanotube composites |
| 2. Metals nanoparticles: | |
| Au | Biosensors |
| Ag | Antimicrobial |
| Au/Ag nanorods | Security bar codes |
| Al | Rocket fuel |
| Si | Displays |
| Fe, activated carbon | Drug delivery systems |
| 3. Oxide nanoparticles: | |
| TiO ₂ | Sunscreens, photovoltaic cells |
| Al ₂ O ₃ nanowires | Purification fillers |
| Silicas (porous) | Delivery systems |
| CeO ₂ | Fuel additive |
| Lu-doped oxides | Phosphors |
| 4. Other inorganic nanoparticles: | |
| Talc, CaCO ₃ | Nanocomposites |
| BaCO ₃ | Coatings filler |
| Ln phosphates | Security and printing |
| Ca phosphates | Bone replacement |
| Clays | Nanocomposites |
| Zeolites | Catalysis |
| SiC | Ceramics |
| 5. Group II-VI quantum dots and wires: | |
| CdSe | Biosensors |
| CdSe and Si | Photovoltaic cells |
| 6. Organics: | |
| Nanocrystals | Delivery systems |
| Dendrimers | Delivery systems |
| Nanoemulsions | Delivery systems |
| Lipid vesicles | Delivery systems |

2.3 Nanomaterials

The prefix 'nano' in nanomaterials mean as small as one billionth of a meter ³ i.e. 10^{-9} m. Matter with any one of the dimension (i.e. length, width or height) that fall into the nanometer scale is considered as a nanomaterial ⁸. They can be metals, clays, semiconductors, polymeric materials and even composites materials. Although widespread interest in this field is recent, but nanomaterials have actually been produced and utilized by mankind for hundreds of year. It started with the use of purple Cassius (coated gold colloids) as a pigment in glass in the middle of 17th century by Andreus Cassius ⁸. However, it was only known in 1857 that the brilliant color was due to the metallic gold nanoparticles ^{1,9}.

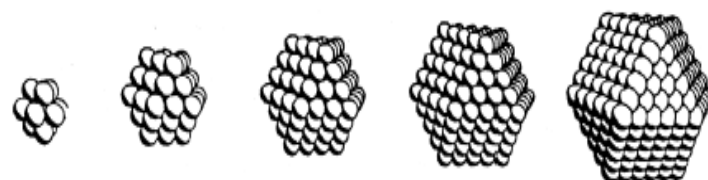
Many terms have been used to describe nanomaterials. In accordance with this, it is important to present some definition of common terminologies used. These are tabulated in Table 2.3.

Table 2.3: Some important terminology used in nanoscience ^{3,10}

| Term | Definition |
|---------------|--|
| Cluster | A collection of units (atoms or reactive molecules) up to about 50 units. |
| Colloid | A stable liquid phase containing particles in the 1-1000 nm range. |
| Nanoparticle | A solid particle in the range of 1-1000 nm that could be nanocrystalline, an aggregate of crystallites, or single crystal. |
| Nanocrystal | A solid particle that is a single crystal in the nanometer size range. |
| Nanocomposite | A combination of two or more phases containing different compositions, where one of the phases is in the nanoscale regime |
| Quantum dot | A particle that exhibits a size quantization effect in at least one dimension. |

What is so special about these nanomaterials? How do they bring about the revolution for future science and technology? When a bulk matter is reduced into submicron size, as the diameter is decrease toward De Broglie wavelength, electrons tend to accumulate onto the surface of matter and these will cause the changes in their properties which are known as the quantum size effect. These enhance and or unique properties exhibited therefore promise a wider and better performance or applications as compared to their bulk entities.

When a particle becomes smaller, the proportion of the surface atoms increases. For example, a nanoparticle with a diameter of 10 nm would have about 10% of its atoms on the surface, whereas nanoparticle with a diameter of 1 nm will expose all its atoms on the surface of the nanoparticle ¹¹. However, for bulk materials the percentage of the surface atoms is almost negligible as compared to the total number of atoms. Hence, the small feature size ensures that more proportions of the metal are exposed at the surfaces that is accessible for exploitation of scientific or technology purposes. Figure 2.1 shows the relation between the total number of atoms in full shell clusters and the percentage of surface atoms.



| Full-Shell "Magic Number" Clusters | 1 | 2 | 3 | 4 | 5 |
|------------------------------------|-----------------|-----------------|------------------|------------------|------------------|
| Number of shells | 1 | 2 | 3 | 4 | 5 |
| Number of atoms in cluster | M ₁₃ | M ₅₅ | M ₁₄₇ | M ₃₀₉ | M ₅₆₁ |
| Percentage surface atoms | 92% | 76% | 63% | 52% | 45% |

Figure 2.1: The relation between the total number of atoms in full shell clusters and the percentage of surface atoms ¹²

As the particle is downsized, its electronic properties start to change. When the wavelength of the electron is of the same order as the particle size itself, it will exhibit properties that lie between its bulk and atoms or molecules. These properties are the so-called quantum size effects as mentioned earlier¹¹. As shown in Figure 2.2, the electronic band structure is no longer continuous from the bulk metal to molecule via nanoparticle. The energy changes from broad or diffusely overlapping HOMO and LUMO in the bulk matter (Figure 2.2(c)) to discrete bands in the atom or molecule (Figure 2.2(a)). For nanosized particles, they exhibit a refined band structure with a combination of both distinct and continuous energy bands. The excitation of the electron between the band gaps is what causes the nanoparticles to reveal a surface plasmon resonance (SPR) band in UV-vis spectroscopy.

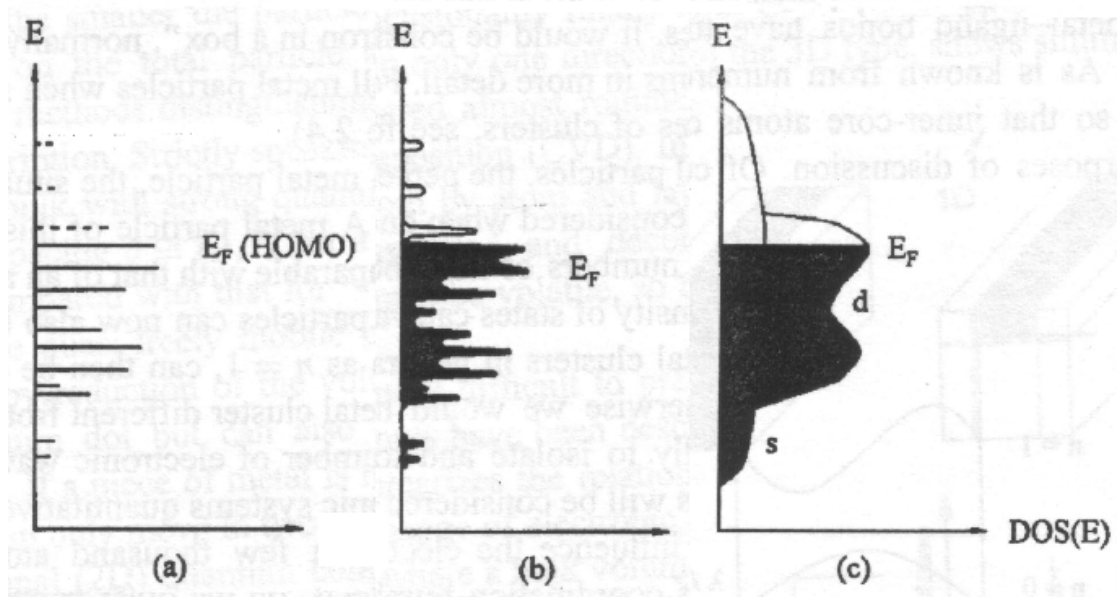


Figure 2.2: Formation of a band structure (a) from a molecular state, (b) from a nanosized particle and (c) the fully developed band structure consisting of s and d band³ (E = energy, E_F = Fermi energy, DOS = density of states)

2.4 Nanoparticles; Preparation, Size and Morphology

There are generally two approaches for the preparation of nanoparticles: top-down and bottom-up³. Top-down methods reduce bulk precursor to micron or nanosize particles often via physical routes such as mechanical milling and the likes, while the bottom-up methods start with atoms/molecules that aggregate in solution or even in gas phase to form particles of definite size under appropriate experimental conditions. The bottom-up routes employ the chemical methods which is a much better route to synthesize uniform particles with distinct size, shape and structure. Chemical reduction using sodium borohydride, hydrazine or alcohol, sol-gel process, pyrolysis, UV or microwave irradiation, ultrasonic agitation are some of the common preparative chemical techniques that are used to prepare nanoparticles. It is known that different size and shape of the nanoparticles will give rise to diverse properties; therefore, one of the main objectives in nanoscience research is to synthesize nanoparticles with the desired size and shape.

2.5 Additives/Stabilizers/Matrices/Supports

The properties of nanomaterials are strongly dependent on their size, morphology and preparative method¹³. In order to control these features, additives or stabilizers such as surfactants, polymers, ligands and dendrimers or matrices and inorganic supports are usually included in the preparative procedure. Basically, nanoparticles can be protected and stabilized by stabilizers against aggregation by two modes – electrostatic (charged or inorganic) and steric repulsion as shown in Figure 2.3^{12,14}. However, matrices or supports have different modes of stabilizing where they will “wrap” the particles in a solution thus preventing particle sintering and aggregation¹⁵.

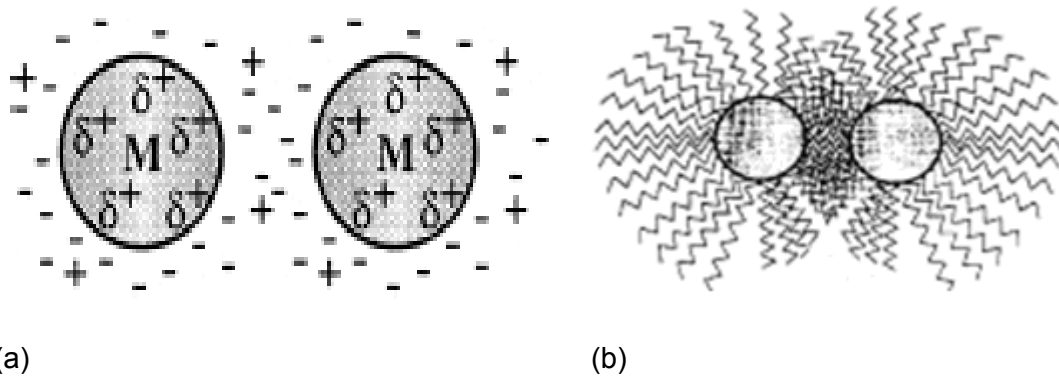


Figure 2.3: Mechanisms of the stabilization of nanoclusters by (a) electrostatic and (b) steric repulsion ¹²

2.5.1. Surfactants

Surfactants are amphiphilic molecules consisting of hydrophilic (likes water) and hydrophobic (fears water) components ¹. When two immiscible phases is mixed with surfactants with the concentration above critical micelle concentration (CMC), surfactants aggregate into structures called micelles, where the hydrophobic end of the molecules is directed into the oil phase whereas the hydrophilic end into the aqueous phase. It can be used to stabilize particles by trapping the metal or metal oxide nanocluster inside the micelle. Various types of microstructures can be formed, namely spherical micelles, cylindrical micelles and lamellar micelles (Figure 2.4) ¹⁶. The size and shape of the nanoparticles will be restricted by the size and structure of the micelles. Some examples of surfactants used are cetyltrimethylammonium bromide (CTAB), sodium lauryl sulfate (SLS), triton X-100 and sodium dodecyl sulfate (SDS) ¹⁷.

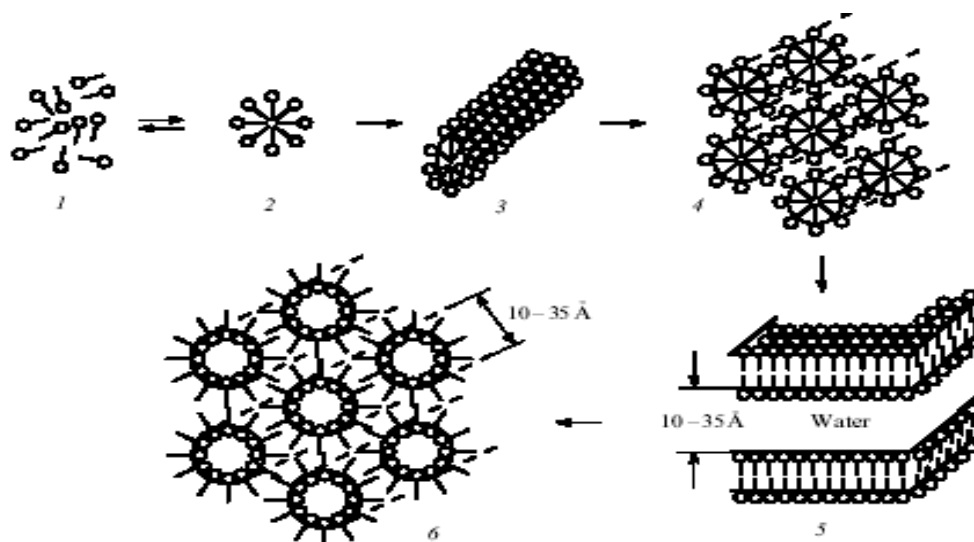


Figure 2.4: Microstructure arising from surfactant (1) monomers, (2) spherical micelle, (3-4) cylindrical micelle, (5) lamellar micelle and (6) water droplets packed as hexagons in the reverse micellar system ¹⁶

2.5.2. Polymers

Polymer refers to a large molecule formed by joining together repeating units of small molecules called monomers ¹⁸. The mechanism for the stabilization of polymer-metal nanoparticles can be summarized into three steps ¹⁴:

- (i) before the reduction of metal nanoparticles, metal ions coordinate to the functional group of the polymers and form complexes
- (ii) during the formation of zero valence metals (reduction) or metal oxides (oxidation), the particles coordinate weakly to the polymers. The coordination ability is dependent on the type of metal or metal oxide and the functional group of polymers.
- (iii) after the formation of the respective colloids, polymers act as stabilizers. The hydrophilic ends are adsorbed on the surface of the particles while the hydrophobic ends formed a barrier surrounding the metal particles to protect it.

Both synthetic and natural polymers have been used as the stabilizers. Polyvinylpyrrolidone (PVP)¹⁹⁻²¹, poly(styrene)-block-poly(2-vinylpyridine)²², poly(vinyl alcohol) (PVA)²³, poly-N-vinylcaprolactam (PVCL)²¹, chitosan²⁴, epoxidized natural rubber (ENR)²⁵ and natural rubber latex²⁶ are some of the examples.

2.5.3. Ligands

A molecule, ion or atom that is attached to the central atom of a coordination compound or other complex is defined as ligand²⁷. Essentially, ligands bear donor group that possess atom(s) with lone-pair electrons. Examples are phosphine, phosphinite, phosphonite, pyridine, oxazoline²⁸ and thiol²⁹. Complexation between the donor atom of the ligand and the central metal atom/ion thus stabilizes the metal or metal oxide nanoparticles. It has been said that the ligand stabilized metal colloids are stable over a period of time under the exclusion of moisture and air³⁰.

2.5.4. Dendrimers

Dendrimers are another type of stabilizer, which is rarely used as compared to ligands or polymers. They are known as a highly bulky oligomer that consists of both internal and peripheral functional groups that provide sites for the metal ions³¹. Poly(amidoamine) dendrimers (Figure 2.5), have been used to stabilize gold, copper, platinum and palladium colloids³¹⁻³⁴. Grohn et al.³² used a different generation of poly(amidoamine) (PAMAM) dendrimer to prepare gold colloids. They concluded that these dendrimers not only prevent the aggregation of metal colloids but also determine their morphologies.

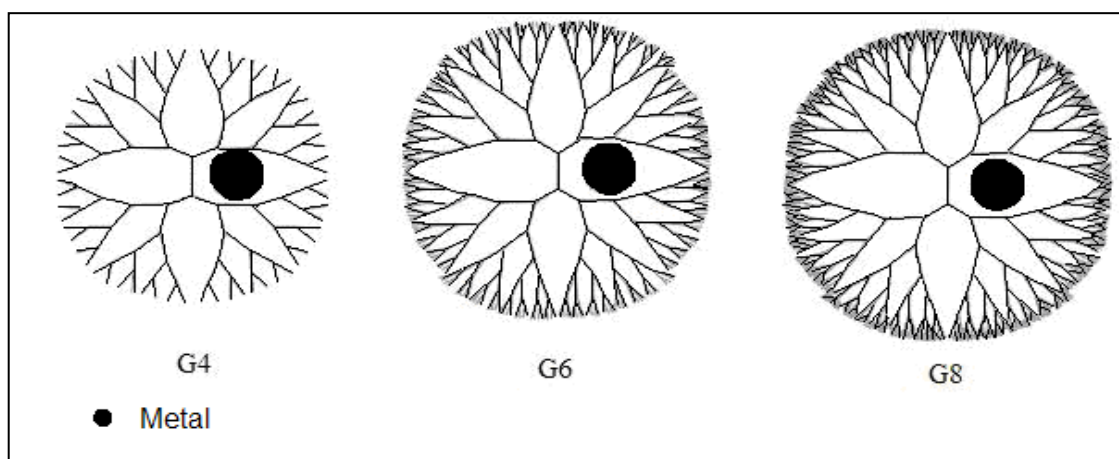


Figure 2.5: Various generation (G4, G6, G8) of poly(amidoamine) dendrimers ³⁴

2.5.5. Matrices/Supports

Nanoparticles can be immobilized in/on the matrices or supports without strong interactions occurring between them ³⁵. Polymer matrices or resins differ from the conventional inorganic supports such as titania, silica and alumina. The nanosized particles are not just simply dispersed on the surface of the supports as in common cases of the inorganic supports; however they are mostly embedded in the polymer matrices, thus preventing the occurrence of particle aggregation.

2.6 Application of Nanomaterials

Application of nanomaterials, at present, cover a wide field including biomedical, electronics and magnetics, superadsorbents, sensors, separations, pigments, catalysis and so on.

2.6.1. Catalysts

Nanoparticle catalysts are perhaps the first nanomaterials widely applied in industries. Nanosize catalysts are always believed to exhibit higher reactivity and selectivity as compared to its bulk catalysts. This is attributed to the followings; ³⁴

- (a). Large surface area-to-volume ratio
- (b). High surface concentrations of corner and edge atoms
- (c). Low coordination numbers of surface atoms
- (d). Unique electronic properties

Many reports have been published regarding the application of nanoparticles in catalysis. For example, gold-chitosan nanocomposites have been used as catalysts for the elimination of active radical species³⁶, colloidal gold sol is the preferred catalyst for glucose's oxidation³⁷ and vinyl polymer-stabilized platinum nanoparticles have been used as catalyst for the hydrogenation of allyl alcohol³⁸.

2.6.2. Biomedical Applications

Application of nanotechnology in medicine has promised a more efficient, effective and healthy life. Particles in nano-form are allowed to "solubilize" into our bloodstream, thus biomolecules that carry nanosized medication can be easily passed through our bloodstream for purposes of cure, diagnosis or therapy. Apart from that, biological tests become quicker and more sensitive when certain nanoparticles are put to work as tags or labels³.

2.6.3. Electronic and Magnetic Applications

The unique properties of nanomaterials owing to the quantum size effects give rise to the fabrication of nano-devices that are suitable for use in electronic and magnetic applications. They are utilized as electroluminescent devices, sensors, information storage media and nanocomputer.^{3,34}

2.6.4. Environmental/Green Chemistry

Below are brief descriptions of some of the examples:

- Adsorbents

Non-porous nanoparticles with large surface area as well as high surface reactivity are efficient adsorbents. Liao and Chen ³⁹ have successfully prepared a novel magnetic nano-adsorbent composite of polyacrylic acid (PAA) and magnetite nanoparticles. The PAA-Fe₃O₄ nano-adsorbent is an efficient composite material for the recovery of lysozyme.

- Water Purification

Contamination of groundwater can be solved using porous metal powder-sand membranes. Iron and zinc nanoparticles have shown high reactivity toward the removal of chlorocarbons in aqueous media ³.

- Solar Cells

Solar energy is a renewable energy. The utilization of solar energy is of particular importance with reference to fossil fuel depletion. The performance of solar cells can be improved by addition of semiconductor nanoparticles in the system. Torre et al. ⁴⁰ have reported that silicon nanoparticles improve the energy conversion in the solar cell.

2.7 Metal Oxides

2.7.1. Importance of Metal Oxides

Various properties of metal oxides such as magnetic, optical, mechanical, electrical, refractory and the likes have been put to use. Most of the transition metal oxides display a range of colours which is suitable for application as pigment. Cerium oxide, CeO₂ for example is a yellow pigment ⁴¹. Metal oxides also exhibit a range of electronic properties from insulators (e.g. Na₂O) to semiconductors (e.g. Fe₃O₄) to nearly metallic conductors (e.g. RuO₂) ⁴². Most of the metal oxides are refractory materials with high melting point that exceeds 1000 °C which can be used as crucible materials ⁴¹.

2.7.2. General Synthetic Routes to Metal Oxide Nanoparticles

There are few known methods to produce metal oxide nanoparticles that are generally common. In this section, magnetite is used as a typical example.

(a). Precipitation Method

Essentially, the preparation of metal oxides can be divided into two types: i.e. either the generation of the metal oxide directly or production of appropriate intermediates which require further processing (such as calcinations and drying) ⁴³. This latter method involves suitable metal salts oxidation in aqueous or non-aqueous medium using precipitating agents. Occasionally, high temperatures are required to produce crystalline products. For example, Cheng et al. ⁴⁴ has successfully synthesized high biocompatibility, non-polymer coated magnetite nanoparticles via ferric and ferrous ions co-precipitation method. These composites are potential materials for clinical diagnosis applications.

(b). Sol-Gel Method ⁴³

Conventionally, sol-gel processing refers to the hydrolysis and condensation of metal alkoxide. This technique did not gain sufficient attention until the work of Geffcken and Berger in 1930s. The sol-gel process can be divided into six steps as depicted schematically in Figure 2.6. This method had been proven versatile. Thus, agglomeration, surface oxidation and sintering between, for example, the hematite particles synthesized can be prevented by coating with silica, titania and the likes. as well as varying others experimental parameters⁴⁵.

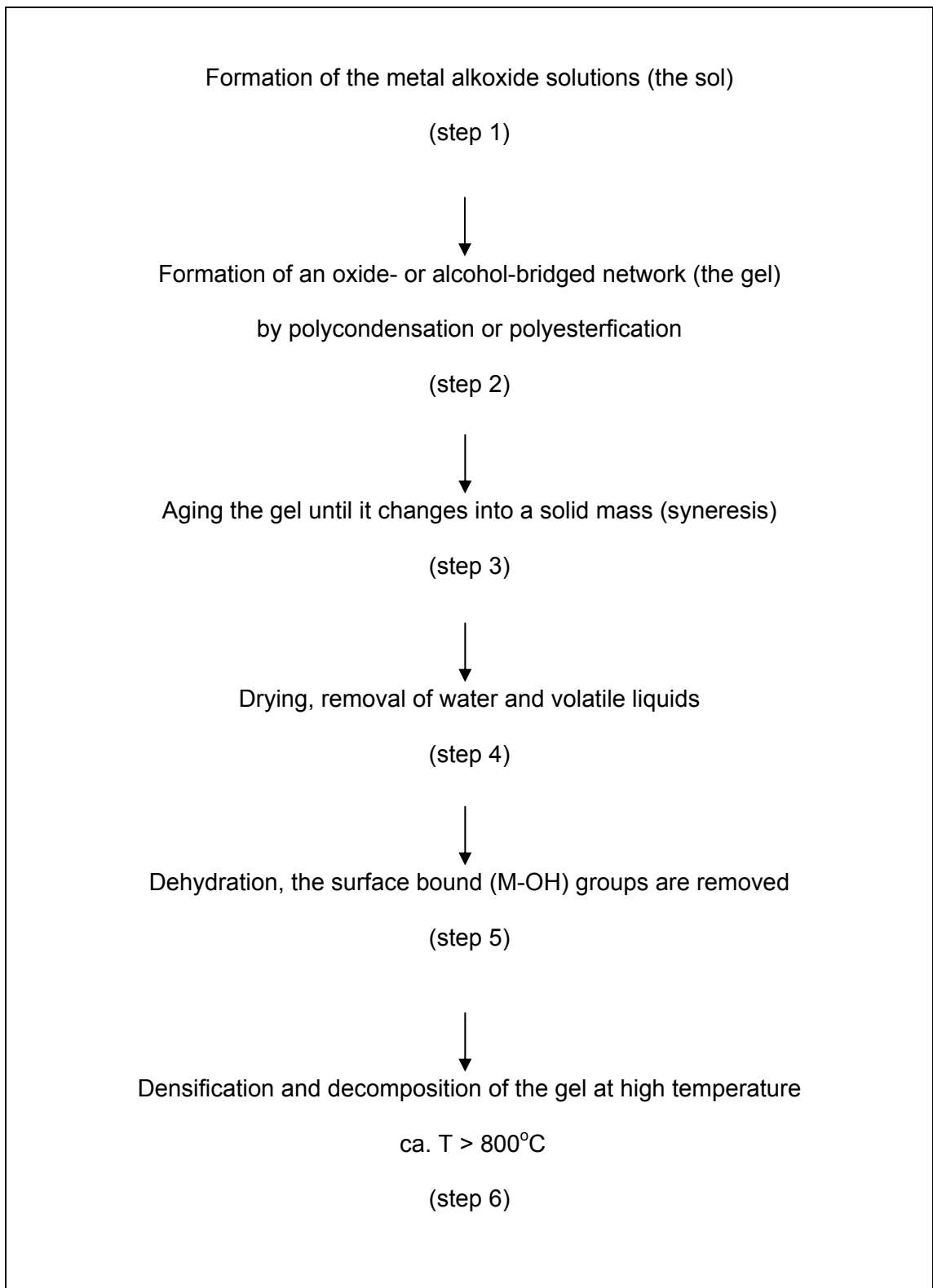


Figure 2.6: Typical steps for sol-gel process ⁴³

(c). Microemulsion Method

Microemulsions are formed when a combination of water, oil, surfactant and co-surfactant are stirred together. The micelle cores created act as a template for particles to grow, therefore controlling the size of the synthesized particles. The size of these cores is dependent on the molar ratio of water to surfactant, w ¹⁷. This thus creates a means to control particle size. This is illustrated by the Schulman's model for the water-in-oil micelle as in Figure 2.7. The radius, r_2 for the outer shield is surrounded by the surfactants and co-surfactants. They provide a barrier to prevent aggregation between the particles. As for the size of the particles they are restricted by radius, r_1 where the prepared particles will have a diameter that is less than $2r_2$. For example, iron oxides synthesis via precipitation in microemulsion were said to have the size ranging from 1 to 20 nm⁴⁶.

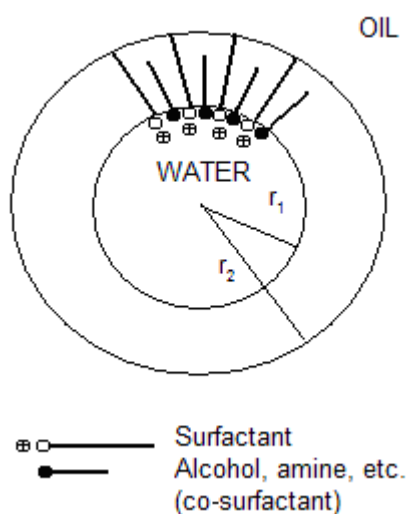


Figure 2.7: Schulman's model for the reverse micelle⁴³

(d). Solvothermal/Hydrothermal Method

Chemical reactions under high pressure and temperature above the boiling point of the solvent used in a sealed vessel are referred to solvothermal reaction process⁴³. If the solvent used is water the process is appropriately termed as

hydrothermal. The metal oxide nanoparticles produced by solvothermal techniques are usually crystalline. Hou et al.⁴⁷ successfully prepared 8 to 11 nm magnetite nanoparticles through a solvothermal reduction technique employing ethylene glycol as the solvent.

(e). Sonochemical Reduction Method

Sonochemical reduction is one of the earliest techniques used to prepare nanoparticles. It involves ultrasound irradiation (frequency range 20 kHz – 10 MHz) that can break the chemical bonding of the precursors⁴⁸. Kim et al.⁴⁹ demonstrated the advantages of sonochemical method versus the conventional co-precipitation method of preparing iron oxide nanoparticles. They found that the magnetite particles synthesized by sonication showed higher crystallinity and are smaller in size.

(f). Pyrolysis Method

Pyrolysis method involves a thermal process in the synthesis of nanoparticles. The thermal process can be aerosol decomposition, evaporative decomposition, spray roasting or spray calcinations⁵⁰. The particles prepared by pyrolysis agglomerate less and are of high crystallinity as compared to sol-gel and precipitation methods. However, the morphology of the particles is difficult to control via this method. Recently, Xu et al.⁵¹ developed citrate pyrolysis techniques to synthesize iron oxide nanoparticles. They found that the initial step of the spontaneous combustion during the decomposition process is the key factor for preparing the nanosized metal oxide particles.

2.8 Iron Oxides

Iron, is one of the most abundant elements in earth's crust⁴². It exists mostly in the form of natural compound as oxide compounds. Iron oxides are widely spread in the global system, including atmosphere, lithosphere and pedosphere. According to

Cornell and Schwertmann ⁵², there are 17 types of iron oxides ranging from oxides, oxyhydroxides and hydroxides. These are as summarized in Table 2.4.

Iron oxides have been utilized for over 30,000 years. Primitive society used red and yellow iron oxides as colorants for paintings. Today, the role of iron oxides as industrial pigment still remains. Apart from that, they have found wide applications in other fields such as catalysts, jewellery, adsorbents, batteries, electrodes, medicine, fertilizers and also as the raw materials for iron and steel industry ⁵².

Table 2.4: Various iron oxides ⁵²

| | |
|------------------|---|
| Oxides | α -Fe ₂ O ₃ ; Hematite Fe ₃ O ₄ ; Magnetite γ -Fe ₂ O ₃ ; Maghemite β - Fe ₂ O ₃ ϵ - Fe ₂ O ₃ FeO; Wustite |
| Oxide-hydroxides | α -FeOOH; Goethite γ -FeOOH; Lepidocrocite β -FeOOH; Akagetite Fe ₁₆ O ₁₆ (OH) _y (SO ₄) _z .nH ₂ O; Schwertmannite δ -FeOOH δ' -FeOOH; Feroxyhyte FeOOH (High pressure) Fe ₅ HO ₈ .4H ₂ O; Ferrihydrite |
| Hydroxides | Fe(OH) ₃ ; Bernalite Fe(OH) ₂ Fe _x ⁱⁱⁱ Fe _y ⁱⁱ (OH) _{3x+2y-z} (A ⁻) _z [A ⁻ =Cl ⁻ ; 0.5 SO ₄ ⁻²]; Green rust |

2.8.1. Properties of Iron Oxides

(a). Magnetic Properties

Iron oxides display various magnetic order such as ferromagnetism, antiferromagnetism and ferrimagnetism depending on the alignment of the electron spin. Bulk magnetite matters are ferromagnetic materials⁵². It will cause the magnetic moment in neighboring atoms to align, induce by the coupling forces, resulting in a large magnetic field. They will become paramagnetic only when the thermal energy is sufficient to overcome the coupling force. However, magnetite particles with a diameter of below 15 nm exhibit superparamagnetism⁴³. The magnetic moments are randomly oriented even at low temperatures. This phenomena promise the stability and dispersion of the magnetic fluids upon the removal of external magnetic field. The superparamagnetic behavior of iron oxides nanoparticles makes it a useful compound that can be applied in clinical magnetic resonance imaging (MRI)⁵³.

(b). Electrical Properties

Most iron oxides fall into the class of semiconductor. The band gap energy between the valence and conduction band is less than 5 eV. To initialize the excitation of electron across the band gap, an external energy such as visible light of appropriate wavelength is needed. Among all the iron oxides, magnetite display almost metallic electrical properties. At room temperature, it shows resistivity in the range of 10^{-4} to 10^9 Ωm . Under the electric field, the electron of ferrous ion can “hop” to the adjacent ferric ion thus forms the conduction current⁵⁴. The oxidation state of ferric and ferrous ions can always be interchanged as common oxidation-reduction reaction (equation (2.1)).



Basically, the electrical conductivity of a material is contributed by ionic conductivity (σ_i) and or electronic conductivity (σ_e). The difference between these